Near-Infrared Fluorescent Dye-Doped Semiconducting Polymer Dots

Yuhui Jin, Fangmao Ye, Maxwell Zeigler, Changfeng Wu, and Daniel T. Chiu*

Department of Chemistry, University of Washington, Seattle, Washington, 98195 United States

ABSTRACT Near-infrared (NIR) fluorescence sensing is desirable for *in vivo* biological measurements, but the method is currently limited by the availability of NIR fluorescent markers as well as by their poor performance, such as self-aggregation and dim fluorescence, in a physiological environment. To address this issue, this paper describes a NIR fluorescent polymer dot (Pdot) that emits at 777 nm. This Pdot was comparable in size to a water-soluble NIR quantum dot that emits at 800 nm (ITK Qdot800) but was about four times brighter and with a narrower emission peak. We formed the NIR Pdot by doping the NIR dye, silicon 2,3-naphthalocyanine bis(trihexylsilyloxide) (NIR775), into the matrix of poly (9,9-dioctylfluorene-co-benzothiadiazole) (PFBT) as the Pdot formed using a nanoscale precipitation technique. Free molecules of NIR775 aggregate in aqueous solution, but encapsulating them into the hydrophobic Pdot matrix effectively introduced them into aqueous solution for use in biological studies. Most importantly, the brightness of NIR775 was dramatically enhanced because of the excellent light-harvesting ability of PFBT and the very efficient energy transfer from PFBT to NIR775. We anticipate this bright NIR Pdot will be useful in biological measurements and cellular imaging where strong NIR emission is beneficial.

KEYWORDS: near-infrared fluorescence · semiconducting polymer nanoparticles · Pdots · energy transfer · large stokes shift · *in vivo* imaging

Application of near-infrared (NIR) fluorescence in biology enormously enhances the sensitivity of *in vivo* measurements and optical imaging[1−7] because monitoring NIR fluorescence minimizes interference from autofluorescence in biological tissues.[3] The most prevalent NIR fluorescent markers are organic dyes, such as cyanines and phthalocyanines.[7−10] The NIR spectra of these organic molecules are determined by the length of their $\pi-\pi$ conjugation structures. Based on this principle, various NIR dyes of different emission wavelengths have been designed and synthesized for bioimaging and diagnosis.[9,10] However, the direct employment of NIR dyes in bioimaging is still challenging for several reasons. First, the large conjugation system of NIR dyes makes them floppy and thus decreases their quantum yield. At the same time, the conjugation system also increases the hydrophobicity of these dyes and induces self-aggregation in aqueous solution, which in combination with the low quantum yield dramatically reduces the brightness of NIR dyes in a physiological environment.[11] Second, these dye molecules require sophisticated chemical modifications to create functional groups for attaching them to biological targeting entities, such as antibodies and proteins. Currently, only a few functionalized NIR dyes are commercially available for bioconjugation. Finally, most NIR dyes, such as phthalocyanines, have a small Stokes shift, which can cause crosstalk between the excitation light and the resulting fluorescence signals.

One method to tackle these challenges is to encapsulate NIR dyes into nanoparticles, which can trap and stabilize NIR dyes inside their matrices without aggregation.[5,12,13] Additionally, the surface of NIR dye-doped nanoparticles can be easily modified with targeting molecules. For example, indocyanine green (ICG) dyes were doped inside calcium phosphate nanoparticles for *in vivo* imaging of human breast cancer.[5,13] The nanoparticle encapsulation enhanced the quantum yield and photostability of the doped ICG dyes and also improved the retention and permeability of the NIR dyes during deep tissue imaging. Other nanomaterials, such as silica nanoparticles and polymer nanoparticles, were also employed to trap NIR dyes and improve their performance, including their photostability.[12,14] However, these encapsulating nanomaterials simply functioned as carriers and surface modifiers and did not fundamentally improve the fluorescence property of NIR dyes.

Semiconducting polymer dots (Pdots) represent a new class of highly fluorescent nanomaterials, which we believe provide the ideal matrix for entrapping NIR dyes.[15−25] Pdots retain the fluorescence properties of their bulk counterparts, the semiconducting polymers, which possess large absorption cross-sections and highly efficient quantum yields.[15,19,24] We recently reported Pdot bioconjugates and clickable Pdots for specific

* Address correspondence to chiu@chem.washington.edu.

Received for review December 3, 2010 and accepted January 18, 2011.

Published online January 31, 2011
10.1021/nn103304m

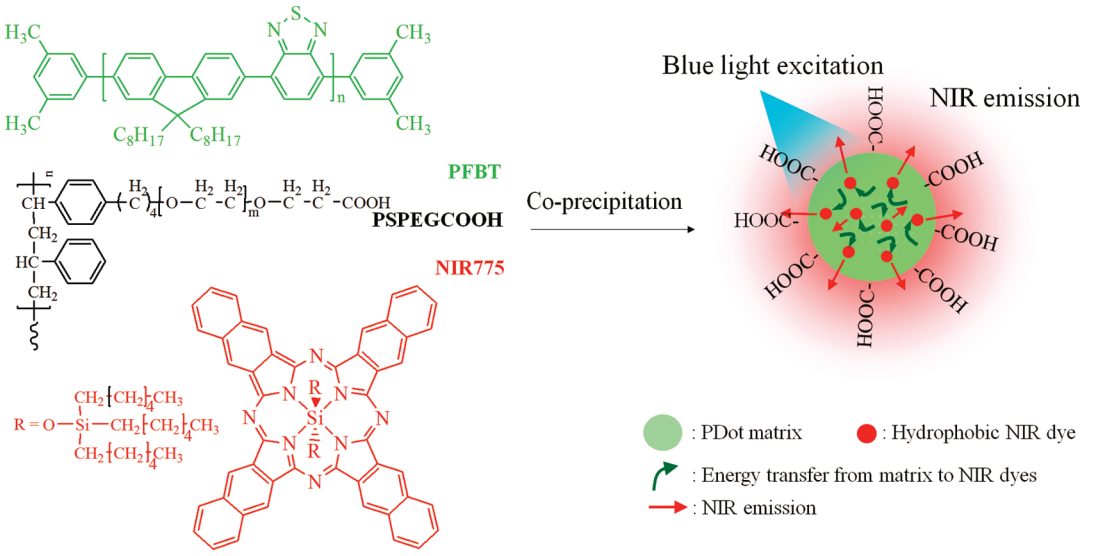

Scheme 1. Preparation of NIR dye-doped Pdots using a nanoscale precipitation technique. Semiconducting polymer PFBT, amphiphilic polymer PS-PEG-COOH, and NIR775 dyes were mixed together in THF and then coprecipitated in water under sonication to form NIR775 dye-doped PFBT Pdots. The Pdot matrix can absorb blue light and transfer the energy to the doped NIR dyes (indicated by green arrows), which then emit strong NIR fluorescence (indicated by red arrows).

cellular targeting.[23,24] However, Pdots made from these polymers can so far only fluoresce in the visible range. Doping organic NIR dyes into Pdots can modulate the fluorescence properties of Pdots and extend their emissions into the NIR region. In this case, we take advantage of the highly efficient energy transfer from the excited Pdot matrix to the doped dyes that are in close proximity to the semiconducting polymer. This efficient energy transfer quenches the fluorescence from the Pdot matrix and enhances the brightness of the dye dopant. Therefore, Pdots not only stabilize the hydrophobic dyes and serve as functionalization agents for bioconjugation but also act as efficient light-harvesting agents that transfer their energy to the doped dyes to improve their fluorescence brightness.

In principle, this strategy can be used to generate a panel of dye-doped Pdots that emit at different wavelengths by varying either the Pdot matrix or the dopant. For emission in the NIR region, we screened a number of NIR dyes (Figure S1, Supporting Information) and found silicon 2,3-naphthalocyanine bis(trihexylsilyloxide) (NIR775) offered the best performance. We also found poly (9,9-dioctylfluorene-co-benzothiadiazole) (PFBT) to be an excellent matrix that offered a large Stokes shift (excitation max at 457 nm and emission max at 777 nm), which reduced the crosstalk between the excitation source and the NIR fluorescence emission. Importantly, Pdots have exceptionally large two-photon absorption cross-sections,[25] and thus it is possible to employ NIR775-doped PFBT Pdots for *in vivo* imaging in which two-photon excitation is used in combination with NIR detection. Here, we describe the optical performance and physical stability of this bright NIR nanoparticle.

RESULTS AND DISCUSSION

Preparation of NIR Dye-Doped Pdots. Scheme 1 illustrates our strategy for preparing NIR-emitting dye-doped Pdots where we encapsulated NIR775 into the matrix of PFBT Pdots using the nanoprecipitation method. PFBT formed the hydrophobic core of the Pdot and served as a host for the NIR dyes. The surface of the Pdot was also functionalized with carboxyl groups by blending PFBT with a carboxyl-functionalized amphiphilic polymer (PS-PEG-COOH) during Pdot formation, which provided the Pdot with a hydrophilic surface as well as an abundance of functional groups for further bioconjugation.

NIR775 fluoresces in hydrophobic solvents, but its fluorescence is greatly diminished in aqueous environments due to self-aggregation.[11] The aggregation was significantly reduced when these dyes were doped inside the Pdot matrix during nanoprecipitation. We chose the nanoscale precipitation approach because of its simplicity, good reproducibility, and ability to form small Pdots with excellent photophysical properties. In this method, we simply dissolved all the components for forming the dye-doped Pdots in anhydrous THF and then injected the THF solution into buffer to form the Pdots under sonication. This sudden change of solvent environment, together with vigorous sonication, led to the formation of nanometer-sized semiconducting polymer particles and simultaneously entrapped the hydrophobic NIR dye (NIR775) within the Pdot matrix. The carboxylate surface was also generated as the amphiphilic polymer, PS-PEG-COOH, embedded its hydrophobic portion within the hydrophobic core of the Pdot while exposing its hydrophilic functional groups at the surface of the Pdots.

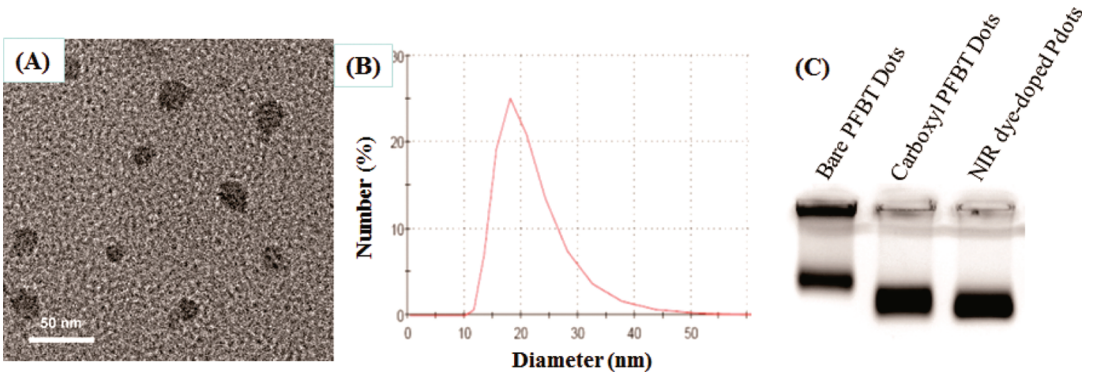

Figure 1. Characterization of NIR775 dye-doped PFBT Pdots. (A) TEM image of NIR775 dye-doped Pdots; the average diameter of the Pdots was 18 nm. (B) Average diameter of NIR775 dye-doped Pdots measured by DLS. (C) Electrophoresis of bare PFBT dots, carboxyl PFBT dots, and NIR dye-doped PFBT Pdots ran in an agarose gel containing 0.7% of agarose and 0.2% of PEG under an applied field strength of 10 V/cm in 20 mM HEPES for 15 min. Bare PFBT dots ran slower because they lacked surface carboxyl groups; carboxyl PFBT dots and NIR dye-doped PFBT Pdots both contained carboxyl groups on their surfaces so they ran faster.

Both transmission electron microscopy (TEM) imaging and the dynamic light scattering (DLS) measurements of the NIR dye-doped Pdots indicated they were quite monodispersed with an average diameter of 18 nm (Figure 1). We verified that the NIR dyes were successfully encapsulated within the Pdot matrix by the following experiments: First, the Pdot solution was filtrated with a 100 K molecular weight cutoff centrifugal membrane, which only allowed free NIR dyes to pass through but not the doped ones that were held inside the Pdots. After filtration, we found the filtrate did not contain NIR dyes as monitored by UV−vis; the absorbance of NIR dye was clearly evident in the solution that contained the NIR dye-doped Pdots (Figure S2, Supporting Information). This result suggests NIR dyes were completely associated with the Pdots. Furthermore, the surface of Pdots was functionalized with carboxylate groups from the amphiphilic polymer PS-PEG-COOH. This surface functionalization significantly decreased the ζ potential of the Pdots from −35.4 mV (bare PFBT dots) to −46.0 mV (Pdots with PS-PEG-COOH coating). Gel electrophoresis also showed the carboxylate Pdots moved much faster than the bare PFBT Pdots of similar size toward the positive electrode (Figure 1C). The NIR dye doping did not affect the ζ potential of the carboxylate Pdots, suggesting that the majority of NIR dyes were only located inside the Pdots and not on the surface.

Modulating Fluorescence Spectra of Pdots. Pdots are notable for their extraordinary fluorescence properties, such as efficient light harvesting and high brightness.[19,24] Pdots with various fluorescence emissions (from blue to red) have been developed using different semiconducting polymers. However, in the context of *in vivo* biological applications, NIR emissions are often needed. But NIR is a wavelength region in which Pdots currently do not emit. It is conceivable that semiconducting polymers can be designed and synthesized to create NIR-emitting Pdots, and we are actively pursuing this approach. Unfortunately, this direction has yet to yield a Pdot with good emission properties in the NIR. But conventional NIR dyes usually have poor water solubility and are prone to aggregation in an aqueous environment, which have so far hindered the direct employment of NIR dyes in biological applications. As a result, we thought doping NIR dyes in Pdots offered a simple and effective way to overcome both challenges as well as to take advantage of the NIR dyes that are currently available.

By directly contacting the semiconducting polymer matrix, NIR dyes were able to efficiently receive energy from the matrix and shift the Pdot fluorescence to the NIR region. We chose the green fluorescent polymer (PFBT) as the host and the phathalocyanine dye (NIR775) as the guest. PFBT is a semiconducting polymer that can be conveniently excited in the blue wavelength region (*e.g.*, 457 or 488 nm) and emits fluorescence at 546 nm. NIR775 exhibits strong NIR fluorescence (777 nm peak) in a hydrophobic environment. As mentioned before, the hydrophobic nature of the NIR dye molecules was important in their stable entrapment inside the hydrophobic Pdot matrix. Moreover, once inside the PFBT matrix, NIR775 received energy from PFBT and converted it into NIR fluorescence more efficiently than other NIR dyes we screened (Figure S1, Supporting Information). The excitation and emission spectra of free NIR775 dye molecules in THF, PFBT Pdots, and NIR775-doped PFBT Pdots in 20 mM HEPES buffer indicated that energy was transferred efficiently from the PFBT matrix to the doped NIR775 and that the fluorescence emission of PFBT dot could be modulated using NIR dye doping (Figure 2).

We found NIR775 efficiently quenched Pdot fluorescence even at a low concentration. Figure 3A shows the reduction in Pdot fluorescence as the concentration of NIR775 was increased from 0.2 to 2%. The intensity of NIR emission of the Pdot-NIR775 was also modulated as the concentration of NIR775 was varied.

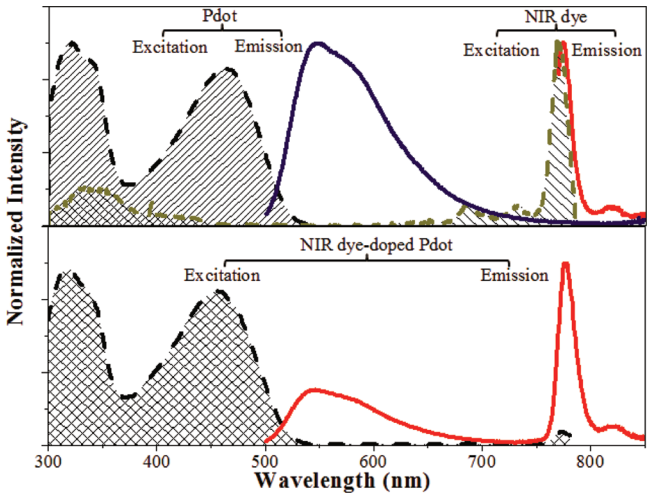

Figure 2. Excitation and emission spectra of PFBT Pdots in 20 mM of HEPES buffer, free NIR775 dyes in THF, and NIR775 dye-doped Pdots in 20 mM of HEPES buffer. The upper panel shows the excitation spectrum of PFBT dots (black dashed line with shadow), excitation spectrum of NIR775 dyes (dark-yellow dashed line with shadow), emission spectrum of PFBT dots (blue solid line), and emission spectrum of NIR775 dyes (red solid line). The lower panel shows the excitation (black dashed line with shadow) and the emission (red solid line) spectra of 0.2% NIR775 dye-doped Pdots.

Doping high concentrations of NIR775 into the Pdot matrix resulted in a decrease in NIR fluorescence because of self-quenching of the NIR dyes (Figure 3E). On balance, we found the best concentration range for dye doping to be 0.2−1%, which offered strong NIR fluorescence.

Energy Transfer from Pdot Matrix to NIR Dyes. One important underlying reason for the high NIR emission we observed from Pdot-NIR775 is the amplified energy transfer exhibited by Pdots. Semiconducting polymers, such as PFBT, are constructed of numerous fluorescent residues that form a large conjugated system. This structure allows the excitons to move along the polymer chain until they encounter a quencher molecule. This migration of excitons facilitates the energy transfer from the polymer to the dopants over even relatively long distances.[15,21,26] For example, for poly(9, 9-dihexylfluorene) Pdots the exciton diffusion distance has been simulated to be around 8 ± 1 nm.[15] In our system, similarly, even a small doping concentration of 2% w/w (which corresponds to an average of 27 NIR dyes per Pdot) of NIR dyes was sufficient to quench the polymer fluorescence by over 95%. Additionally, the hydrophobic nature of the dye and the Pdot matrix ensured close interaction between the acceptor dye and the donor matrix, which also enhanced efficient energy transfer.

We examined the quenching efficiency using the Stern−Volmer equation (eq 1):[26]

$$F_0/F = 1 + K_{sv}[A] \quad (1)$$

where F_0 and F represent the fluorescence intensity of donor without and with the acceptor, respectively. The value [A] stands for the concentration of the acceptor, and K_{sv} is the Stern−Volmer quenching constant. Figure 3D shows that our experimental results were in good agreement with the Stern−Volmer relationship. The K_{sv} value indicates that one NIR775 dye molecule could potentially quench six PFBT polymer chains in the Pdot, confirming the amplified energy transfer from PFBT to NIR775.

We also measured the change in the fluorescence lifetime of the Pdots before and after the doping of NIR dyes. The lifetime of PFBT dots was initially 2.4 ns, which decreased to 1.2 ns after doping with 0.2% of NIR775 into Pdot matrix (Figure 3C). At 0.2% doping concentration, the fluorescence quantum yield of PFBT at 540 nm also dropped from 0.368 to 0.08 (Table 1).

Accompanying the quenching of PFBT fluorescence was a concomitant generation of NIR emission. The amplified energy-transfer process was further favored by the large extinction coefficient of the NIR dye (5.2×10^5 $M^{-1}cm^{-1}$). As a result, we observed highly efficient energy transfer despite the poor spectral overlap between the PFBT's fluorescence and the NIR775's absorbance (Figure 3B). We calculated the Förster radius (R_0) of the pair to be 3.7 nm. The quantum yield of the NIR emission from PFBT−NIR775 was around 0.11 (Table 1).

Fluorescence Enhancement. The fluorescence intensity of NIR775 was greatly enhanced because of Pdot doping. When excited at 457 nm in aqueous solution, the PFBT−NIR775 exhibited 40 times stronger fluorescence over the equivalent amount of free NIR dye excited at 763 nm in THF, an organic solvent in which NIR775 is well dispersed (Figure 4A). The improvement was even greater if an aqueous solution was used instead. Such a large enhancement is attributed to the excellent light-harvesting ability of PFBT and the efficient energy transfer to the NIR dyes.

The hydrophobic core of the host Pdot matrix also provided an excellent hydrophobic environment that stabilized NIR775. The absorbance spectrum of NIR775

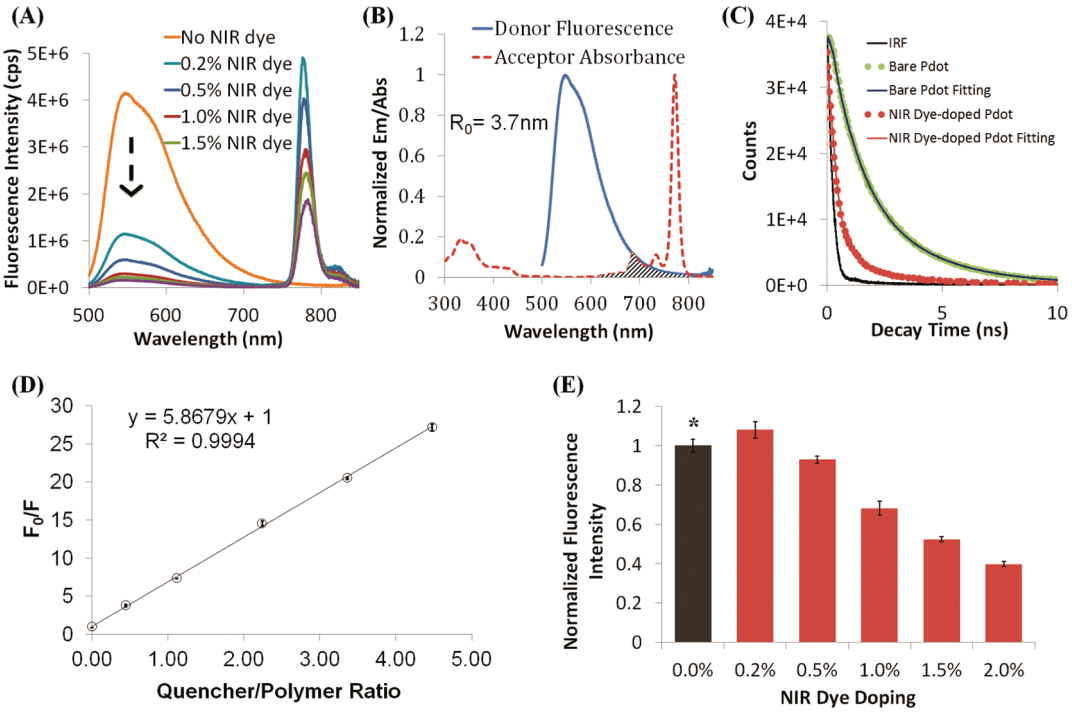

Figure 3. Fluorescence properties of NIR775 dye-doped PFBT Pdots. (A) Fluorescence spectra of NIR775-doped PFBT Pdots at different doping concentrations presented as the weight percentage of NIR775 in the Pdot. (B) Spectral overlap between the normalized emission spectrum of PFBT Pdot (donor) and the normalized absorption spectrum of NIR775 (acceptor); the calculated Förster radius between the donor and acceptor (R_0) is 3.7 nm. (C) Fluorescence lifetime measurements of PFBT Pdots and NIR775-doped PFBT Pdots. The lifetime of bare PFBT Pdots is 2.4 ns (experimental data: green dots; fitting: blue solid line), which is reduced to 1.2 ns after doping with 0.2% of NIR775 dyes (experimental data: red dots; fitting: red solid line). Black solid line represents the internal reference (IRF). (D) Quenching of NIR775 in Pdot matrix. The ratio of the fluorescence intensity of the original Pdots without dye doping (F_0) and with NIR775 doping (F) is proportional to the concentration of the dopant (hollow dots with error bar). Data were fit with the Stern−Volmer equation (solid line). (E) Fluorescence intensity of NIR775-doped PFBT Pdots as a function of dopant concentration. The black column with asterisk represents the 546 nm emission of PFBT Pdots without dye doping.

TABLE 1. Fluorescence Quantum Yield of NIR775 Dyes, PFBT Pdots, and NIR775 Dye-Doped PFBT Pdots

	NIR dye in THF	NIR dye-doped PS dots	PFBT dots	0.2% NIR775 dye-doped PFBT Pdots
PFBT emission	n/a	n/a	0.368	0.080
NIR775 emission	0.07	0.07	n/a	0.110

doped in Pdot and dispersed in water was similar to the spectrum of free NIR dyes dissolved in THF, which indicated the dyes did not aggregate inside the Pdots as the free NIR dyes would do if exposed to an aqueous environment (Figure S2, Supporting Information). In addition, the quantum yield of the doped NIR dyes was 0.11 in the PFBT matrix and 0.07 in a polystyrene matrix, which was fairly close to the 0.07 value of free NIR dyes measured in THF (Table 1). This result indicates the doped NIR dyes were free of aggregation. If they were not, then a much reduced quantum yield would have been observed.

The excellent light-harvesting efficiency and amplified energy transfer offered by Pdots allowed us to design a bright NIR emitting PFBT−NIR775 Pdot with a large Stokes shift (excitation peak: 457 nm; emission peak: 777 nm) that is difficult to achieve with traditional dye molecules (Figure 2). To understand the enhancement offered by the Pdot matrix, we carried out a control experiment in which we employed a hydrophobic matrix made of polystyrene (PS) instead of PFBT for doping NIR775; aside from the change in polymer matrix, all other parameters of the experiment remained constant. The PS matrix can stabilize NIR dyes and prevent them from aggregation, similar to the PFBT matrix, but PS cannot harvest light or transfer energy to the doped NIR dyes. The fluorescence of the NIR775-doped PS dots excited at 763 nm was over 100 times dimer than the PFBT−NIR775 Pdots excited at 450 nm (Figure 4A). Additionally, NIR775-doped PS dots cannot be efficiently excited at 450 nm as anticipated. Both PS and PFBT offer an excellent hydrophobic matrix for hosting NIR775, but this experiment shows clearly the advantages of light harvesting and amplified energy transfer offered only by Pdots.

Brightness of PFBT-NIR775. We found the NIR775-doped PFBT Pdots possessed very strong NIR fluorescence that was much brighter than conventional dyes. As mentioned before, on a per molecule basis, NIR775 molecules doped in Pdots were about 40 times brighter than free NIR775 molecules dissolved in an organic solvent. On a per particle basis, the emission intensity

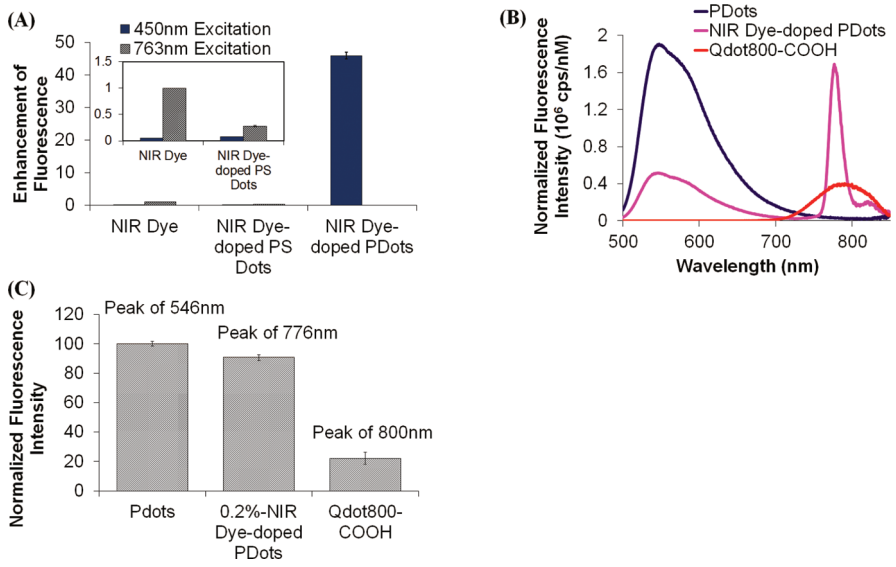

Figure 4. Fluorescence enhancement of NIR775 doped inside PFBT Pdot matrix. (A) Normalized fluorescence peak intensities of free NIR775 dyes, NIR775 dyes doped in PS dots, and NIR775 doped in PFBT Pdots. For PFBT Pdots, excitation was at 450 nm (blue columns), and for free NIR775 and NIR775 doped in PS, excitation was at 763 nm (black patterned columns). The fluorescence of free NIR dyes was measured in THF, while the others were measured in 20 mM HEPES buffer (pH 7.4). (B) Fluorescence emission intensities, using identical particle concentration, of bare PFBT Pdots, NIR775-doped Pdots, and Qdot800. (C) The peak fluorescence intensity of bare PFBT Pdots, NIR775-doped Pdots, and Qdot800 normalized by the particle concentration.

of the NIR775-doped PFBT Pdots was comparable to bare Pdots without dye doping and was several times brighter than NIR quantum dots (Qdot800 from Invitrogen, Inc.). For example, NIR775-doped PFBT Pdots had about four times more intense fluorescence than Qdot800 (Figure 4C). In addition to being brighter, NIR775-doped PFBT Pdots also had a much narrower fluorescence emission spectrum than Qdot800 (Figure 4B).

Given the intense fluorescence in the NIR, the large Stokes shift that minimizes crosstalk between excitation light and NIR fluorescence emission, and the narrow emission spectrum, we anticipate NIR775-PFBT Pdots will find applications in molecular detection and cellular imaging. In additional to improving the optical properties of NIR dyes, their encapsulation into Pdots also allows for easy functionalization and bioconjugation. Therefore, we believe the strategy we outlined here can be broadly applied to improving the performance and versatility of a wide range of other NIR dyes.

Stability of PFBT-NIR775. One concern we had with dye-doped Pdots was the potential for the doped dyes to leak out from the Pdots. In this scenario, the energy transfer from the Pdot to the dyes would be reduced and would decrease the NIR emission peak. To examine this potential issue, we monitored the normalized NIR fluorescence of 0.2% NIR775-doped PFBT Pdots in 20 mM of HEPES buffer for 72 h (blue striped columns in Figure 5). Because the NIR dye-doped Pdots may be attractive for *in vivo* applications, we also carried out the leakage test in human blood plasma at 37 °C for 72 h. Again, we did not observe any noticeable leakage (red cross-hatched columns in Figure 5). These results

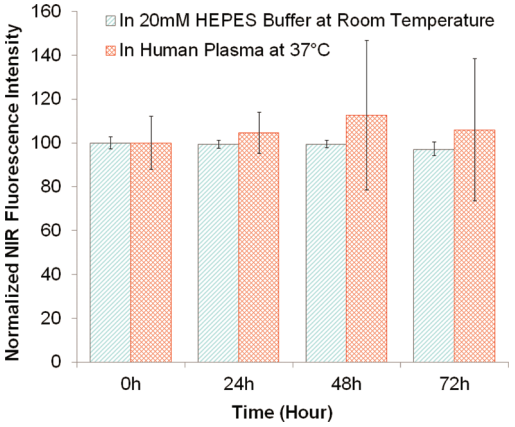

Figure 5. Studies of potential leakage of NIR775 dye dopant from PFBT Pdots. The leakage of 0.2% NIR dye-doped Pdots was tested both at room temperature in 20 mM HEPES buffer (pH 7.4, blue striped columns) and at 37 °C in human blood plasma (red cross-hatched columns).

indicate that the hydrophobic NIR dyes were tightly and stably held within the hydrophobic Pdot core and did not leak into the aqueous solution under our experimental conditions.

CONCLUSIONS

This paper describes a versatile and simple method for tuning the fluorescence properties of Pdots by doping the hydrophobic matrix of Pdots with hydrophobic dyes. This strategy offers several important advantages: (1) The hydrophobic matrix of Pdots effectively disperses and stabilizes the doped dyes and allows the dyes to be used in an aqueous environment;

(2) The functional groups present on the surface of Pdots allow the dye-doped nanoparticles to be labeled with a wide range of biomolecules; (3) Pdots act as extremely efficient light harvesters that greatly enhance the brightness of the doped dyes; and (4) Pdots offer amplified energy transfer to the dopant, thus enabling efficient tuning of the emission properties of Pdots using the dopant. Using this strategy, we have developed a NIR-emitting Pdot that is much brighter than the free dye and also has a narrower emission spectrum than a comparable Qdot. Although potential leakage of the doped dyes from the Pdot matrix was initially a concern, we have demonstrated that the strong hydrophobic interaction between the matrix and the dopant effectively confines the dopant to the Pdot matrix. We anticipate this simple strategy can be generally applied to a broad range of dye dopants as well as Pdots. For *in vivo* imaging, it is important to note that Pdots have exceptionally large two-photon absorption cross-sections, which together with the large Stokes shift demonstrated here makes NIR775-doped PFBT Pdots ideally suited for two-photon imaging, where two-photon excitation is followed by detection in the NIR. The new NIR-emitting Pdot should therefore find broad utility in cellular labeling and *in vivo* fluorescence imaging.

MATERIALS AND METHODS

Materials. Poly[(9,9-dioctylfluorenyl-2,7-diyl)-co-(1,4-benzo-(2,1′,3)-thiadiazole)] (PFBT; MW, 157 000 Da; polydispersity, 3.0) was purchased from ADS Dyes Source, Inc. (Quebec, Canada). Polystyrene (PS) and polystyrene graft ethylene oxide functionalized with carboxyl groups (PS-PEG-COOH; MW 21 700 Da of PS moiety; 1200 Da of PEG-COOH; polydispersity, 1.25) were purchased from Polymer Source Inc. (Quebec, Canada). NIR dye, silicon 2,3-naphthalocyanine bis(trihexylsilyloxide) was purchased from Sigma Aldrich, Inc. (St. Louis, MO). Qdot800-COOH was purchased from Invitrogen Corporation (Carlsbad, CA). Human whole blood was purchased from PlasmaLab International. All the other chemicals were purchased from Sigma Aldrich, Inc. (St. Louis, MO) and used without purification.

Preparation of NIR Dye-Doped Pdots. NIR dye-doped Pdots were prepared using a nanoscale precipitation technique. In a typical procedure, a tetrahydrofuran (THF) solution containing 50 μg/mL of PFBT, 50 μg/mL of PS-PEG-COOH, and 0.2 μg/mL of NIR775 dye was prepared. A 5 mL aliquot of the mixture was then quickly dispersed into 10 mL of water under vigorous sonication. The extra THF was evaporated at an elevated temperature (lower than 100 °C) with the protection of nitrogen gas. The THF-free Pdot solution was filtrated through a 0.2 μm cellulose membrane filter and adjusted to the appropriate concentration.

Preparation of Control Pdots. Two types of Pdots, PFBT dots (with and without carboxyl functionalization) and NIR dye-doped polystyrene dots (PS dots), were prepared as controls using the aforementioned nanoscale precipitation method. A THF solution containing PFBT or PFBT and PS-PEG-COOH was injected into water to produce PFBT dots with or without carboxyl groups. Similarly, PS instead of PFBT was mixed with NIR dyes and PS-PEG-COOH in THF for preparing the NIR dye-doped PS dots. The rest of the protocol and conditions was kept unchanged for the preparation of Pdots.

Characterization of Pdots. The size and morphology of the Pdots were investigated using TEM (FEI Tecnai F20, 200 kV). TEM samples were prepared by dripping the Pdot solution onto a carbon-supported copper grid (FEI Tecnai, Inc.) and drying it at room temperature before observation. The hydrodynamic size of the Pdots was also measured in aqueous solution using a DLS instrument (Malvern Zetasizer Nano ZS). UV−vis absorption spectra of Pdots and NIR dyes were taken in water with a DU 720 scanning spectrophotometer (Beckman Coulter, Inc., CA). The carboxyl surface of Pdots was verified by measuring the ζ potential using the Malvern Zetasizer. Pdots with and without carboxyl surfaces were also tested in a gel electrophoresis experiment. The gel was prepared using 0.7% of normal melting agarose, 0.2% of PEG (MW 3350), and 20 mM HEPES buffer. The Pdot samples were loaded into the electrophoresis channels with the help of 30% glycerol and run in 20 mM HEPES buffer (pH 7.4) under an applied field strength of 10 V/cm for 15 min using a Mupid-exU submarine electrophoresis system. The gel was then developed using a Kodak image station 440CF system.

Fluorescence Measurements. Fluorescence spectra of Pdots and NIR dyes were taken with a Fluorolog-3 fluorospectrometer (HORIBA JobinYvon, NJ). All the Pdots and PS dots were measured in 20 mM HEPES buffer at the same particle concentration (pH 7.4). The NIR dye-doped pdots and the NIR dye-doped PS dots were excited at 457 nm with a xenon lamp, and the autocorrected emission spectra were recorded from 500 to 850 nm. The free NIR dye in THF and NIR dye-doped PS dots in HEPES buffer were also examined with excitation light of both 457 and 763 nm. Fluorescence lifetime data of NIR dye-doped Pdots and PFBT dots were obtained using a time-correlated single-photon counting instrument (TCSPC). Fluorescence quantum yields of PFBT Pdots and NIR dye-doped Pdots were collected using an integrating sphere (model C9920−02, Hamamatsu Photonics) with a 457-nm excitation from a 150 W CW xenon lamp. The quantum yield of free NIR dye in THF was also measured using 763-nm excitation.

Leakage Test of NIR Dye-Doped Pdots. Potential leakage of NIR dye from the Pdot matrix was studied by tracking the change in the ratio of the acceptor-to-donor fluorescence. The 0.2% NIR dye-doped Pdots were kept at room temperature in 20 mM HEPES buffer (pH 7.4) for three days as well as in blood plasma at 37 °C for three days. Their fluorescence spectra were monitored using a HORIBA Jobin Yvon fluorospectrometer.

Acknowledgment. We gratefully acknowledge support of this work by the National Institutes of Health (CA147837 and NS062725).

Supporting Information Available: The UV−vis absorption spectra of various NIR dye-doped Pdots and NIR775 dye-doped Pdots of different concentrations are shown in the supporting figures. This material is available free of charge *via* the Internet at http://pubs.acs.org.

REFERENCES AND NOTES

1. Kosaka, N.; Ogawa, M.; Choyke, P. L.; Kobayashi, H. Clinical Implications of Near-Infrared Fluorescence Imaging in Cancer. *Future Oncol.* **2009,** *5*, 1501–1511.
2. Kondepati, V.; Heise, H.; Backhaus, J. Recent Applications of Near-Infrared Spectroscopy in Cancer Diagnosis and Therapy. *Anal. Bioanal. Chem.* **2008,** *390*, 125–139.
3. Frangioni, J. V. In Vivo Near-Infrared Fluorescence Imaging. *Curr. Opin. Chem. Biol.* **2003,** *7*, 626–634.
4. Chen, X.; Conti, P. S.; Moats, R. A. In vivo Near-Infrared Fluorescence Imaging of Integrin $\alpha v\beta 3$ in Brain Tumor Xenografts. *Cancer Res.* **2004,** *64*), 8009–8014.
5. Altnoğlu, E. İ.; Adair, J. H. Near Infrared Imaging With Nanoparticles. *Wiley Interdiscip. Rev.: Nanomed. Nanobiotechnol.* **2010,** *2*, 461–477.
6. Sharma, R.; Wendt, J. A.; Rasmussen, J. C.; Adams, K. E.; Marshall, M. V.; Sevick-Muraca, E. M. New Horizons for Imaging Lymphatic Function. *Ann. N.Y. Acad. Sci.* **2008,** *1131*, 13–36.

7. Achilefu, S. The Insatiable Quest for Near-Infrared Fluorescent Probes for Molecular Imaging. *Angew. Chem., Int. Ed.* **2010,** *49*, 9816–9818.
8. Nesterova, I. V.; Verdree, V. T.; Pakhomov, S.; Strickler, K. L.; Allen, M. W.; Hammer, R. P.; Soper, S. A. Metallo-Phthalocyanine Near-IR Fluorophores: Oligonucleotide Conjugates and Their Applications in PCR Assays. *Bioconjug. Chem.* **2007,** *18*, 2159–2168.
9. Peng, X.; Draney, D. R.; Volcheck, W. M.; Bashford, G. R.; Lamb, D. T.; Grone, D. L.; Zhang, Y.; Johnson, C. M. In *Phthalocyanine Dye As an Extremely Photostable and Highly Fluorescent Near-Infrared Labeling Reagent*; Samuel, A., Darryl, J. B., Ramesh, R., Eds.; SPIE: Bellingham, WA, 2006; p 60970E.
10. Kovar, J. L.; Simpson, M. A.; Schutz-Geschwender, A.; Olive, D. M. A Systematic Approach to The Development of Fluorescent Contrast Agents for Optical Imaging of Mouse Cancer Models. *Anal. Biochem.* **2007,** *367*, 1–12.
11. Brasseur, N.; Nguyen, T.-L.; Langlois, R.; Ouellet, R.; Marengo, S.; Houde, D.; van Lier, J. E. Synthesis and Photodynamic Activities of Silicon 2,3-Naphthalocyanine Derivatives. *J. Med. Chem.* **1994,** *37*, 415–420.
12. Deng, T.; Li, J. S.; Jiang, J. H.; Shen, G. L.; Yu, R. Q. Preparation of Near-IR Fluorescent Nanoparticles for Fluorescence-Anisotropy-Based Immunoagglutination Assay in Whole Blood. *Adv. Func. Mater.* **2006,** *16*, 2147–2155.
13. Altnoğlu, E. I.; Russin, T. J.; Kaiser, J. M.; Barth, B. M.; Eklund, P. C.; Kester, M.; Adair, J. H. Near-Infrared Emitting Fluorophore-Doped Calcium Phosphate Nanoparticles for In Vivo Imaging of Human Breast Cancer. *ACS Nano* **2008,** *2*, 2075–2084.
14. Kumar, R.; Ohulchanskyy, T. Y.; Roy, I.; Gupta, S. K.; Borek, C.; Thompson, M. E.; Prasad, P. N. Near-Infrared Phosphorescent Polymeric Nanomicelles: Efficient Optical Probes for Tumor Imaging and Detection. *ACS Appl. Mater. Interfaces* **2009,** *1*, 1474–1481.
15. Wu, C.; Zheng, Y.; Szymanski, C.; McNeill, J. Energy Transfer in a Nanoscale Multichromophoric System: Fluorescent Dye-Doped Conjugated Polymer Nanoparticles. *J. Phys. Chem. C* **2008,** *112*, 1772–1781.
16. Howes, P.; Green, M.; Levitt, J.; Suhling, K.; Hughes, M. Phospholipid Encapsulated Semiconducting Polymer Nanoparticles: Their Use in Cell Imaging and Protein Attachment. *J. Am. Chem. Soc.* **2010,** *132*, 3989–3996.
17. Howes, P.; Thorogate, R.; Green, M.; Jickells, S.; Daniel, B. Synthesis, Characterisation and Intracellular Imaging of PEG Capped BEHP-PPV Nanospheres. *Chem. Commun.* **2009,** 2490–2492.
18. Moon, J.; McDaniel, W.; MacLean, P.; Hancock, L. Live-Cell-Permeable Poly(p-phenylene ethynylene). *Angew. Chem., Inter. Ed.* **2007,** *46*, 8223–8225.
19. Pecher, J.; Mecking, S. Nanoparticles of Conjugated Polymers. *Chem. Rev.* **2010,** *110*, 6260–6279.
20. Tuncel, D.; Demir, H. V. Conjugated Polymer Nanoparticles. *Nanoscale* **2010,** *2*, 484–494.
21. Wu, C.; Bull, B.; Christensen, K.; McNeill, J. Ratiometric Single-Nanoparticle Oxygen Sensors for Biological Imaging. *Angew. Chem., Inter. Ed.* **2009,** *48*, 2741–2745.
22. Wu, C.; Bull, B.; Szymanski, C.; Christensen, K.; McNeill, J. Multicolor Conjugated Polymer Dots for Biological Fluorescence Imaging. *ACS Nano* **2008,** *2*, 2415–2423.
23. Wu, C.; Jin, Y.; Schneider, T.; Burnham, D. R.; Smith, P. B.; Chiu, D. T. Ultrabright and Bioorthogonal Labeling of Cellular Targets Using Semiconducting Polymer Dots and Click Chemistry. *Angew. Chem., Inter. Ed.* **2010,** *49*, 1–6.
24. Wu, C.; Schneider, T.; Zeigler, M.; Yu, J.; Schiro, P. G.; Burnham, D. R.; McNeill, J. D.; Chiu, D. T. Bioconjugation of Ultrabright Semiconducting Polymer Dots for Specific Cellular Targeting. *J. Am. Chem. Soc.* **2010,** *132*, 15410–15417.
25. Wu, C.; Szymanski, C.; Cain, Z.; McNeill, J. Conjugated Polymer Dots for Multiphoton Fluorescence Imaging. *J. Am. Chem. Soc.* **2007,** *129*, 12904–12905.
26. Lakowicz, J. R. *Principles of Fluorescence Spectroscopy*, 3rd ed.; Springer Science+Business Media, LLC: New York, 2006; p 960.